Journal of Catalysis **191,** 1–11 (2000)
doi:10.1006/jcat.1999.2801, available online at http://www.idealibrary.com on IDEAL®

Linear Butenes from Isobutene over H-Ferrierite: *In Situ* Studies Using an Oscillating Balance Reactor

Lucía M. Petkovic and Gustavo Larsen[1]

Department of Chemical Engineering, University of Nebraska—Lincoln, Lincoln, Nebraska 68588-0126

Received April 19, 1999; revised November 19, 1999; accepted November 23, 1999

The transformation of isobutene into linear butenes was studied by means of a packed-bed configured oscillating balance reactor (OBR), *in situ* **diffuse reflectance infrared Fourier-transform spectroscopy (DRIFTS), and mass spectrometry. The zeolite surface becomes covered with oligomeric hydrocarbons within the first few minutes on stream. There are a number of key differences between the isobutene isomerization reaction and the reverse (*n*-butene-to-isobutene) transformation. First, the kinetically controlled regimes of these two reactions are roughly 70 K apart. The difference in apparent activation energies for the two processes (ca. 11 kcal/mol) suggests that the two reactions are likely to proceed via different kinetic pathways. Second, a higher degree of branching in the oligomeric species formed by acid-catalyzed polymerization of isobutene, relative to those from 1-butene, causes a smaller coke precursor critical uptake to effect the site-to-pore blockage transition. The "aging" (hydrogen loss and condensation leading to true coke) of such branched chains is slower than that of chains resulting from a 1-butene feed. The impact of intrazeolitic oligomeric hydrocarbons on both the rate of formation of coke precursors and the isobutene isomerization process is also discussed.**

Key Words: **H-Ferrierite; pulse mass analyzer; coke; oscillating balance reactor; butenes.**

INTRODUCTION

H-Ferrierite is a particularly attractive catalyst for isomerization of linear butenes to isobutene (1–6). The catalytic stability of this system, after its surface has been practically saturated with carbonaceous deposits, is one of its most remarkable features. This has been demonstrated by a number of techniques including the use of conventional chemical quantification and classification of coke deposits (1) and microbalances (2) and, more recently, by means of an oscillating balance reactor (OBR) (3). The latter mimics packed-bed behavior much more accurately than standard microbalance techniques (3, 7–9), and allows for the measurement of oligomeric carbon uptakes in real time and with excellent mass-time resolution. With the aid of this technique, we were able to recently model the impact of coke precursor deposition on both its own formation rate and on the *n*-butene-to-isobutene reaction (3).

Up to about two-thirds of the total oligomeric carbon uptake, linear deactivation (site blockage) models for both the coking and the isomerization reactions were found (3). A transition from a linear to an exponential coking rate decay was evident at higher carbonaceous residue levels, an observation consistent with the occurrence of pore blockage phenomena (10). Used in combination with mass spectrometric detection of products at short times on stream (TOS), and *in situ* diffuse reflectance infrared Fourier-transform spectroscopy (DRIFTS), our OBR results showed that highly saturated oligomers are quickly formed but slowly give way to true coke-like species at longer TOS (3). Andy *et al.* (1) have studied the nature of solvent-extracted coke fractions at different TOS, which enabled these authors to propose a coke formation mechanism involving a complex network connecting a library of polycyclic molecules.

Much less attention has been paid to the reverse reaction, i.e., the formation of linear butenes and cracking products from isobutene. It is generally accepted that linear olefins oligomerize much faster than branched alkenes (11). This reaction has been studied over H-Ferrierite by Guisnet *et al.* (6), but we have reason to believe their data were influenced by mass transfer artifacts as discussed later. Nevertheless, it appears reasonable to speculate that the isobutene-to-*n*-butene reaction does not follow a kinetic pathway merely opposite to that of *n*-butene isomerization (6). The linear butenes are generally treated as a lump since double-bond shift is a facile reaction that frequently allows the three isomers to reach thermodynamic equilibrium.

The primary focus of this contribution is to study the behavior of H-Ferrierite during isobutene isomerization, as monitored by OBR, DRIFTS, and MS experiments, and to compare the results with those for the more practical *n*-butene-to-isobutene transformation (3). Emphasis is placed on the nature of carbonaceous residues deposited on the catalyst and their rate of formation, as well as on the impact that such oligomeric species have on the rate of isobutene isomerization at short and long TOS. Our data

[1] To whom all correspondence should be addressed.

0021-9517/00 $35.00

are finally discussed in terms of the butene isomerization mechanisms that have been previously proposed. As for the latter, controversy still remains as to whether a unimolecular (12), "pore mouth" (13), or other kinetic scheme at the molecular level is responsible for their unique catalysis over H-Ferrierite. When the reaction is carried out under differential reactor regimes and reaction data are collected prior to surface saturation of the H-Ferrierite with oligomeric species, it appears that selective sites for *n*-butene isomerization are lost (instead of being produced) at very short TOS (3). This indicates that such selective sites do not necessarily have to operate at the pore mouths, as previously suggested (1). Recently, Guisnet *et al.* (6b) suggested that at short TOS (i.e., when the H-Ferrierite pores are not yet saturated with oligomeric species) a pseudomonomolecular mechanism involving adsorbed species with tertiary carbenium ion character, instead of benzylic carbocations, might constitute the active site. On the other hand, the pillar of monomolecular alkane and alkene rearrangements has always been the popular protonated cyclopropyl (PCP) intermediates (14, 15). For hydrocarbons smaller than C_5, this picture has long been resisted since it leads to species with strong primary carbenium ion character. Theoretical calculations indicate that, while the stability of adsorbed alkoxy intermediates does not depend strongly on their primary, secondary, or tertiary nature, the energy of potentially relevant transition states is ranked according to a more classic carbenium ion picture (16). Still, when a rate analysis rather than a percentage yield study at high conversions is carried out, it is not immediately obvious that a bimolecular or a pseudomonomolecular kinetic scheme must operate during the isomerization of butenes over H-Ferrierite. For example, Houzvicka and Ponec (4) carried out pulse studies in which controlled amounts of coke well below saturation were deposited stepwise. These authors found that the rate of isomerization of linear butenes never increases with hydrocarbon residue content, in clear contradiction with the results of Guisnet *et al.* (6), which focused on H-Ferrierite that had operated at at high conversion levels for several minutes. Similarly, no rate enhancement was found in the *n*-butene-to-isobutene reaction over H-Ferrierite at low conversions for a range of temperatures and *n*-butene partial pressures (3). Thus, low conversion and low coke content data render support to the idea that there is no adsorbed carbocation involved in the generation of the active site, unlike previously suggested (6).

EXPERIMENTAL

The properties of the H-Ferrierite catalyst used in this study, made from the ammonium form of a commerical material from Tosoh Corporation, are presented elsewhere (3). Likewise, thorough descriptions of the *in situ* DRIFTS apparatus (18), the OBR operation (3, 7–9, 17), and the mass spectrometric detection of products in the OBR outflow (3), can be found elsewhere.

The main feature of commercial OBR units from R&P Company is that they have a very fast reponse to mass transients, and they allow for precise uptake measurements at short TOS. For OBR data to be meaningful, it is necessary to minimize dead volume effects on its response. We have estimated that our reactor manifold design produces unreliable gas flow transients only during the first 7–14 s, and uptake curves were corrected for that effect (3). Typically, 0.05 g catalyst was placed in the oscillating element, and reactions were conducted at a total pressure of 1 atm.

The DRIFTS cell is essentially a flow reactor composed of a temperature-controlled ceramic cup, in which the catalyst powder is packed and gases are allowed to flow through. A Nicolet 20SXB FTIR spectrometer and a commerical DRIFTS cell from Spectratech were employed. To perform MS studies of the OBR effluent, a stainless-steel capillary tube was attached to the OBR outlet, and an MKS residual gas analyzer was used to follow a total of 16 m/e ratios. The MS results complement gas chromatograhy (GC) data, collected with a 8610B gas chromatograph from SRI equipped with a Carbopack C 2-m × 1/8-in. SS packed column from Supelco. In all cases, stainless-steel reaction manifolds with Brooks 5850D mass flow controllers were used.

RESULTS AND DISCUSSION

Preliminary Reaction Tests and General Methodology

Figure 1 shows the standard procedure used to reduce OBR raw data. An equivalent blank run with nonporous

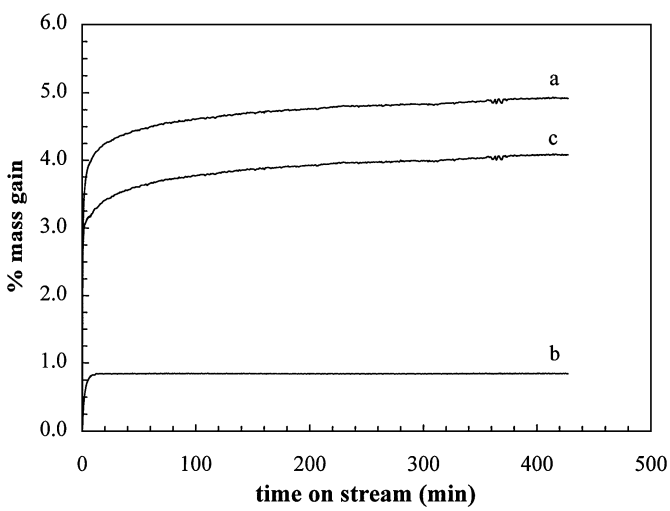

FIG. 1. Mass gain for a H-Ferrierite sample under adsorption/reaction of isobutene at 20.3 kPa and 513 K. WHSV = 37 g isobutene (g cat.)$^{-1}$ h^{-1}, 45 mg H-Ferrierite sample. All curves are corrected for a lag time of 14 s. (a) Raw data for H-Ferrierite. (b) Mass gain for blank. (c) Corrected curve (curve a minus curve b).

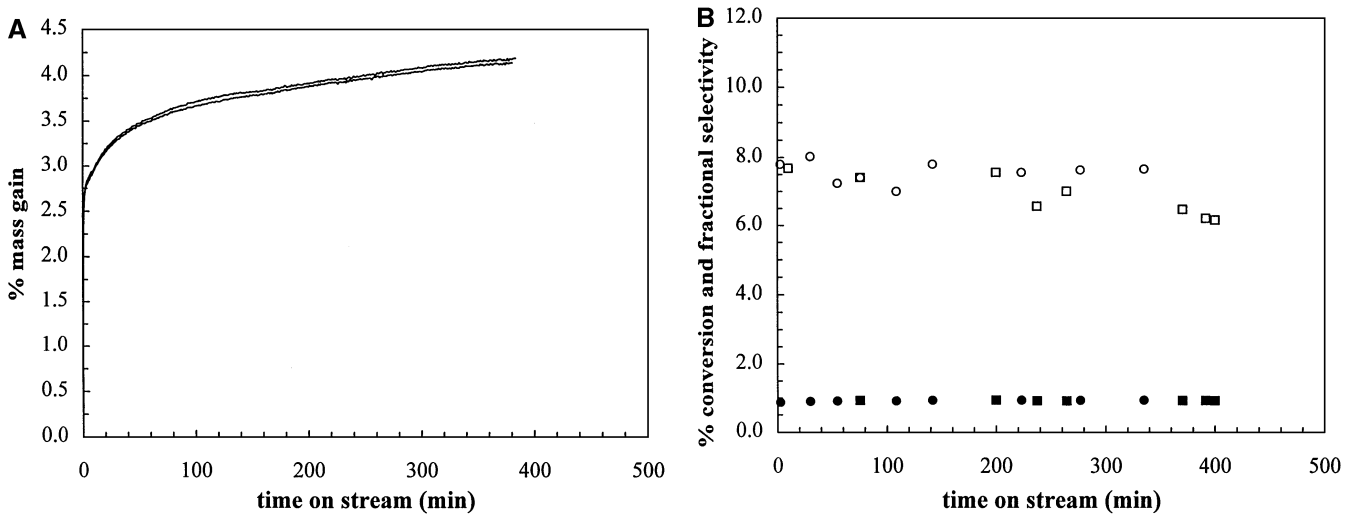

FIG. 2. Results for two experiments separated by a few reaction/regeneration cycles in between. Isobutene at 20.3 kPa and 543 K. WHSV = 37 g isobutene (g cat.)$^{-1}$ h^{-1}, 45 mg H-Ferrierite sample. (A) Corrected mass gain. (B) Catalyst percentage conversion (open symbols) and selectivity as a fraction of one (filled symbols). Squares and circles represent the two experiments.

α-Al_2O_3 or quartz is always necessary to account for mass changes that solely due to gas density change on switching the feed from an inert gas to the reacting mixture. To avoid any potential irreproducibility associated with the repeated loading of the OBR cell with a new catalyst bed, and to test whether the H-Ferrierite catalyst was stable on cycling, two sets of data were collected at the same pressure and temperature, with several reaction/regeneration cycles in between. Within very small error, Fig. 2 shows that the same catalyst bed can be used for the isobutene-to-*n*-butene reaction a number of times, providing a regeneration (calcination) scheme identical to that previously reported for the reverse reaction (3). Catalyst reusability also proved possible for the *n*-butene isomerization reaction as well (3). Throughout this paper, the focus remains on the isobutene isomerization pathway, and only data for the reverse process that have not been reported by our group in Ref. (3) are presented.

Another issue that we viewed as a particularly important one to resolve prior to further data analysis was that of kinetics versus diffusion control. Guisnet *et al.* (6) presented activation energy data for both the forward (to isobutene) and reverse isomerization reactions around 623 K, and in the weight hourly space velocity (WHSV) range 2–70 h^{-1}. Activation energy values of 14 ± 1 and 10 ± 1 kcal/mol for the two reactions, respectively, were reported by these authors, presumably at the high end of their WHSV range to ensure differential reactor operation. Figures 3 and 4 show our own ln(rate)-versus-1/T data measured at comparable WHSV values. The data shown in Figs. 3 and 4 represent catalyst performance at long TOS, i.e., at very high coking levels. The concave-down nature of these curves is taken as clear indication that a transition from kinetic to transport control exists in both these processes. Intuitively, reactions occurring inside partially or totally blocked pores are expected to undergo severe diffusion limitations. In a temperature range that is approximately 100–120 K below that employed by Guisnet *et al.* (6) for the isobutene-to-*n*-butene reaction, we calculated an isobutene isomerization E_a value of 21 kcal/mol. This estimate was obtained by considering the four lowest temperature data points, and it is taken as a reasonably good lower bound for the true apparent activation energy of this process over H-Ferrierite. Liu *et al.* (19) pointed to the fact that temperature control in

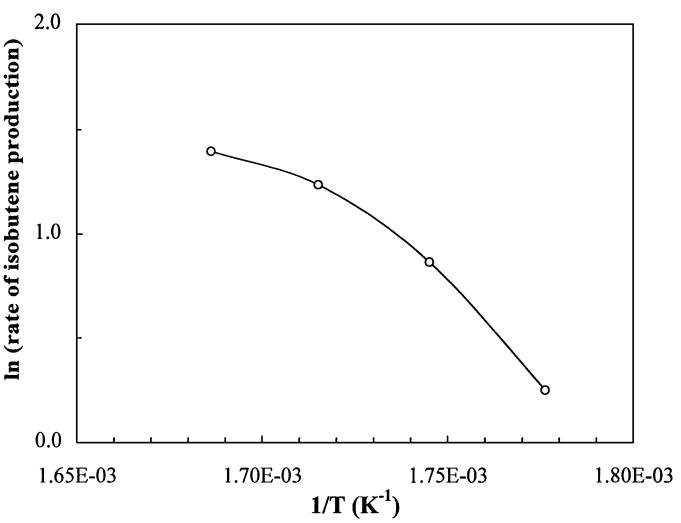

FIG. 3. Arrhenius plot for the skeletal isomerization of isobutene. After 6.5 h TOS. Isobutene in feed at 20.3 kPa. WHSV = 37 g isobutene (g cat.)$^{-1}$ h^{-1}, 45 mg H-Ferrierite sample. Activation energy calculated from slope at the four lowest temperatures, $E_a = 21$ kcal/mol.

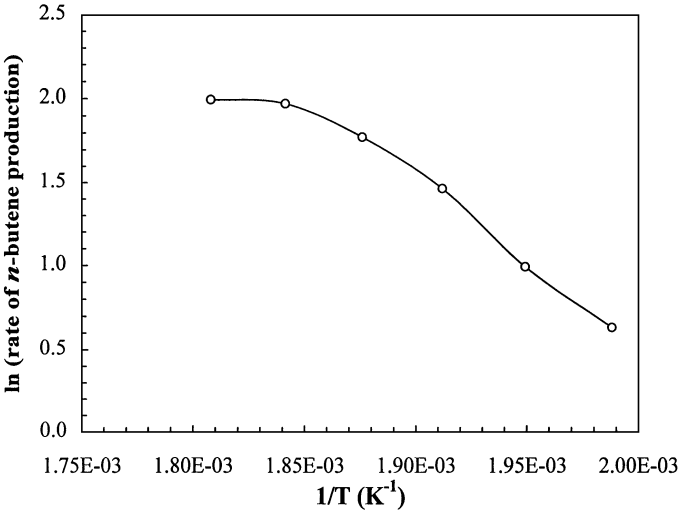

FIG. 4. Arrhenius plot for skeletal isomerization of *n*-butenes. After 4 h TOS. 1-Butene at 101.3 kPa. WHSV = 52 g butene (g cat)$^{-1}$ h^{-1}, 45 mg H-Ferrierite sample. Activation energy calculated from slope at the three lowest temperatures, $E_a = 32$ kcal/mol.

this type of commercial OBR apparatus is done at the wall of the reactor enclosure, instead of directly inside the catalyst bed. These authors measured a temperature difference of 33 K between the catalyst bed and the wall in the range 700–730 K. While we recognize that all of our data, having been taken with wall temperature control, systematically deviate from (but are internally consistent with) the true bed temperature, this still constitutes the most effective experimental approach because insertion of a thermocouple into the oscillating element degrades the S/N ratio of the OBR (19). We have operated the OBR at about temperatures 200 K lower than those used by Liu *et al.* (19) for *n*-heptane reforming, which suggests that a 30 K deviation between bed and wall is likely to represent a worst case scenario. Assuming such deviation, the region that we define as kinetically controlled should roughly be 130–150 K lower than the temperature range employed by Guisnet *et al.* (6) for the isobutene isomerization reaction. Under such assumption, the calculated isobutene isomerization E_a becomes 19 kcal/mol. Nevertheless, being twice as large as the value reported by Guisnet *et al.* (6), we believe that it is the data presented in this paper that more closely represent the kinetic behavior of H-Ferrierite. A similar estimate of E_a for the *n*-butene-to-isobutene transformation from Fig. 4, using the three lowest temperature points, was found to be 32 kcal/mol. The measurement of an "E_a" that is actually half the actual value has long been associated with diffusion control (20). In addition, this large discrepancy is not believed to be due to differences in E_a values that one should expect between fresh and aged H-Ferrierite. It is now apparent from both our work (3) and new results from Guisnet *et al.* (6b) that the E_a data in Ref. (6a) represent values for aged or partially aged H-Ferrierite. In Ref. (6a), the square pulse technique was used to minimize the occurrence of coke deactivation in H-Ferrierite during *n*-butene isomerization, but a waiting (reaction) period of 2 min prior to data collection was allowed. As shown below, and as indicated in Ref. (6b), an unacceptably large fraction of oligomeric hydrocarbon is deposited during the first minute on stream for the data in Ref. (6a) to be considered representative of the performance of fresh H-Ferrierite.

In light of standard Gibbs free energy data, ΔG_f^0 values for the three linear isomers are above that of isobutene by only 2.9 (1-C_4), 1.7 (*cis*-C_4), and 1.4 (*trans*-C_4) kcal/mol (21). Thus, the E_a for isobutene isomerization being lower than that of its reverse reaction by about 11 kcal/mol, it is clear that the forward and reverse skeletal rearrangements of butenes proceed via different kinetic pathways. We are unable at this point to provide a satisfactory explanation for this observation. It is difficult to picture a transition state connecting product and reactant in the isobutene-to-isobutene reaction that cannot be used by the reverse process as well. The reaction order in 1-butene was found to be 0.3, measured at 4 h TOS, and that in isobutene for the reverse reaction was 0.8. Selected TOS data are shown in Fig. 5. In the temperature range in which the isobutene isomerization process can be termed "kinetic," the selectivity toward linear butenes approaches unity, even though trace amounts of disproportionation and hydride transfer products were detected (see Fig. 5). Heavier isomers (C_6–C_8) were not detected by gas chromatography. It must be emphasized that for the isobutene isomerization reaction, which is the main focus of this contribution, the modeling of coke precursor deposition relied on the lowest temperature points shown in Fig. 3.

Tables 1 and 2 show the different butene ratios relative to the experimental equilibrium values reported by Choudary (22). The assumption that all linear butenes are equilibrated

TABLE 1

Comparison of Experimental and Equilibrium Ratios for Butene Isomers[a]

Temp (K)	Equilibrium ratio			Experimental ratio for experiments with 1-butene		
	trans/1	*cis*/1	*cis/trans*	*trans*/1	*cis*/1	*cis/trans*
563	2.8	1.6	0.6	2.4–2.8	1.4–1.9	0.5–0.7
573[b]	2.7	1.6	0.6	2.1–2.9	1.3–1.8	0.6
573[c]	2.7	1.6	0.6	2.4–3.0	1.5–2.1	0.6–0.7
573	2.7	1.6	0.6	2.4–2.6	1.5–1.6	0.6
583	2.6	1.5	0.6	1.9–2.5	1.1–1.5	0.6
593	2.5	1.4	0.6	2.3–2.7	1.6–1.7	0.6–0.7
608	2.4	1.4	0.6	2.3–2.5	1.4–1.6	0.6

[a] Experiments performed at 1-butene partial pressure of 101.3 kPa unless otherwise indicated.

[b] Reactant partial pressure of 33.8 kPa.

[c] Reactant partial pressure of 67.6 kPa.

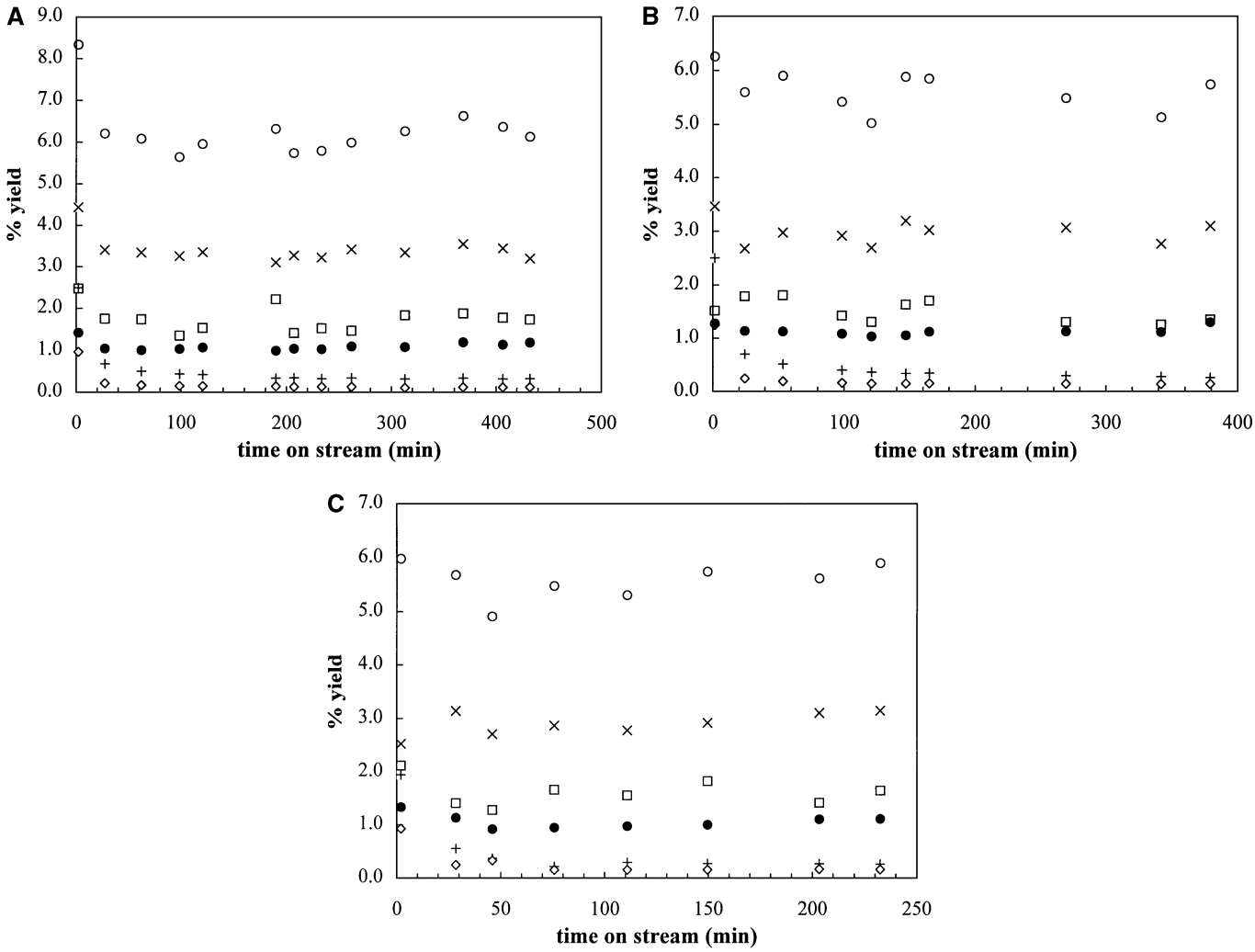

FIG. 5. Product yields for H-Ferrierite catalyst under flowing isobutene at 533 K and partial pressures of (A) 6.8 kPa, (B) 13.5 kPa, and (C) 20.3 kPa. (○) *n*-Butenes as a lump, (×) *trans*-2-butene, (□) *cis*-2-butene, (●) 1-butene, (+) propene, (◇) isobutane. Total feed of 60 cm^3/min, 45 mg H-Ferrierite sample.

over H-Ferrierite appears to hold for the isomerization of 1-butene, a fact that justifies the generic use of the word "*n*-butenes" to represent a feed composed solely of 1-butene. This situation is somewhat different for the isobutene-to-*n*-butene reaction. First, this reaction is run under a kinetic regime that required temperatures ca. 70 K lower than those employed for the isomerization of *n*-butenes. This would favor kinetic rather than thermodynamic control on the double-bond shift network. Second, double-bond shift must occur as secondary reactions from isobutene, i.e., after skeletal rearrangement has taken place. For *n*-butene to isobutene, a monomolecular (4) and two different pseudomonomolecular (6) mechanisms over aged H-Ferrierite have been proposed, but as discussed earlier, an exact inverse path is unlikely to be followed by reverse reaction. A bimolecular pathway for isobutene isomerization would require ß-scission but, for example, theoretical computations performed at different theory levels predict E_a values for this step alone of 60–68 kcal/mol for a zeolite-adsorbed isohexyl alkoxide (16). Generation of linear isomers from two isobutene molecules would involve dimerization, at least one methyl shift, and, finally, ß-scission. Thus, it is conceivable that isobutene follows a unimolecular isomerization pathway (different from that of 1-butene isomerization) that favors formation of 1-butene as primary product. Note that the trend in Table 2 is to favor 1-butene over the other two linear isomers with respect to equilibrium values. It has long been recognized that equilibration of linear isomers via double-bond shift is facile. However, there are clearly two factors that can account for the observation of *cis*-/1- and *trans*-/1- ratios that are lower than those predicted by thermodynamics in the isobutene-to-*n*-butene transformation (see Table 2): the low temperatures necessary to achieve kinetic regimes in the isobutene-to-*n*-butene

TABLE 2

Comparison of Experimental and Equilibrium Ratios for Butene Isomers[a]

Temp (K)	Equilibrium ratio			Experimental ratio for experiments with isobutene		
	trans/1	*cis*/1	*cis/trans*	*trans*/1	*cis*/1	*cis/trans*
503[b]	3.7	2.0	0.5	3.4–3.6	1.5–2.4	0.5–0.7
503[c]	3.7	2.0	0.5	3.1–3.5	1.4–2.7	0.4–0.8
503	3.7	2.0	0.5	1.3–3.8	1.3–2.5	0.4–1.6
513	3.7	2.0	0.5	1.2–3.2	1.2–2.0	0.5–1.2
523	3.5	1.9	0.5	1.5–3.0	1.1–2.0	0.4–0.9
533[b]	3.4	1.8	0.5	2.7–3.3	1.3–2.2	0.4–0.7
533[c]	3.4	1.8	0.5	2.4–3.0	1.1–1.6	0.4–0.7
533	3.4	1.8	0.5	1.9–3.0	1.3–1.8	0.5–0.8
543	3.1	1.8	0.6	2.1–2.9	0.8–1.8	0.3–0.8
553	3.0	1.7	0.6	2.1–2.9	1.2–1.8	0.5–0.7

[a] Experiments performed at isobutene partial pressure of 20.3 kPa unless otherwise indicated.

[b] Reactant partial pressure of 6.8 kPa.

[c] Reactant partial pressure of 13.5 kPa.

reaction relative to those of the reverse process, and (ii) the fact that double-bond shift in linear isomers becomes a secondary reaction that must occur in a reactor operated at low conversions. Even so, there is still the question of why 1-butene, instead of the two internal isomers, is formed preferentially from isobutene prior to double-bond shift equilibration. This might be due to the occurrence of zeolite cage effects that favor the formation of the terminal, less sterically restricted linear isomer as secondary product. Such phenomena would likely be overcome more efficiently in the 1-butene-to-isobutene reaction because of the higher temperatures required for the forward process. Another unresolved issue that still remains is the fact that methyl shifts of alkoxy species resulting from adsorption of olefins on zeolite acid sites are still predicted by theory (16) to be more energy demanding ($E_a = 70$ kcal/mol) than any of the experimentally derived butene skeletal isomerization E_as values reported thus far. A third possibility is either the "pore mouth" catalysis proposed earlier (1), in which delocalized benzylic carbocations act as the alkylating agent, to initate a cycle leading to isomerization. or the tert-butyl cation site (pseudomonomolecular mechanism) proposed at very short TOS (6). Houzvicka and Ponec (4) have criticized such proposal in light of pulse reaction experiments, since these authors were unable to detect an increase in the isomerization rate with controlled increases in the hydrocarbon residue content in H-Ferrierite. In addition, the proposal in Ref. (1) requires "aged" coke; i.e., delocalized benzylic carbocations must form from olefin oligomers after cyclization and hydrogen loss, and that (as discussed in the next sections) can take several hours. Our previous work has shown that "pore mouth" catalysis is not a requirement (3) since selective isomerization sites are lost prior to pore blockage on a time scale that does not permit the oligomeric residues to become true coke. Despite the fact that experimental evidence points to the occurrence of unimolecular mechanisms not involving delocalized benzylic species or other forms of adsorbed hydrocarbons as the actual catalytic site, theoretical calculations are currently under way in our group to gain some insight into Andy and co-workers' (1) intriguing proposal. The key motivation remains the lower experimental energetics of the two butene skeletal isomerization processes relative to theoretical predictions on conventional acidic zeolite–hydrocarbon chemistry.

Coke Precursors: Deposition Rate and Structure

Since coke precursors, in the form of olefin oligomers, are responsible for the total hydrocarbon uptake of H-Ferrierite at very short TOS (3), it is important to realize that the modeling of transients in this paper does not involve the highly unsaturated C_xH_y species we normally associate with "true" coke. As discussed below, formation of the latter is a much slower process despite the fact that, in the interest of adopting a simple nomenclature, we have often elected throughout this paper to call the oligomeric hydrocarbon residues just "coke."

Several empirical forms of coke deposition rates have evolved from the traditional Vohries percentage coke-versus-time approach. In particular, linear self-poisoning of the coking reaction is taken as indicative of site blockage (10),

$$r_c/r_c^0 = 1 - \alpha_1 C_c, \qquad [1]$$

where the subscript c indicates coke (in a loose sense), the superscript o indicates initial rate or rate extrapolated to zero TOS, C_c is the measured coke uptake, and α_1 is a proportionality constant. Similarly, pore blockage is believed to be manifested by an exponential coke self-poisoning dependence (10):

$$r_c/r_c^0 = \exp(-\alpha_1 C_c). \qquad [2]$$

For the *n*-butene isomerization reaction, a transition from linear to an exponential impact of coke amount on its own formation rate was found around 70% total saturation uptake (3). This is likely due a percolation threshold value, above which pore plugging plays a dominant role in the total uptake of oligomeric hydrocarbons.

Figure 6 shows a similar analysis done for the isobutene-to-*n*-butene reaction. A number of observations can be made. First, extrapolation of the linear region suggests that coke levels roughly two to three times smaller than those observed for the *n*-butene isomerization reaction appear to be sufficient to cause the site-to-pore blockage transition. As in our previous study, we interpret the intercept of the *x* axis resulting from extrapolation of the linear region (note that under site blockage regimes, Eq. [1] holds) as the maximum amount of surface hydrocarbon residues on the

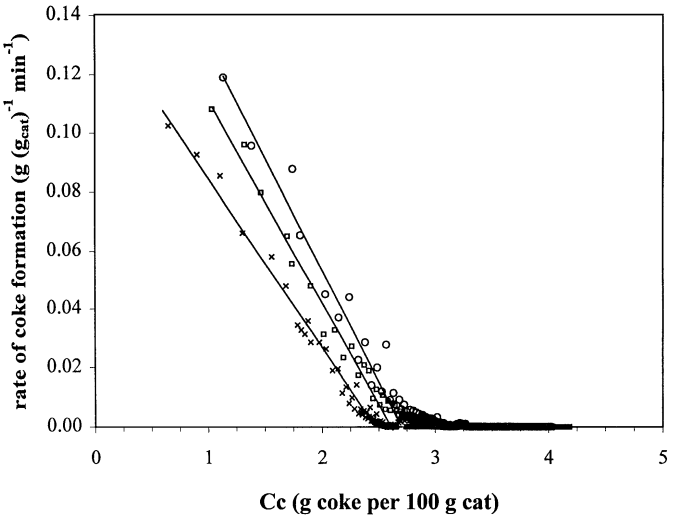

FIG. 6. Rate of coke formation as a function of coke content at 20.3 kPa isobutene partial pressure and reaction temperatures of (○) 513, (□) 523, and (×) 533 K.

catalyst due to site fouling only. For the three different temperatures used in this study, this value appears to be bound between 2.5 and 2.8 wt%. In contrast, the same analysis led to site fouling limits in the range 5.6–7.2 wt% when 1-butene was used as feed instead (3). We take this marked difference as an indication that it is isobutene, rather than the product linear butenes, that accounts for coke deposition phenomena. This view will be supported by our MS results. One possible explanation for this is that the relatively higher degree of branching of oligomers resulting from isobutene is responsible for a more effective pore plugging mechanism, with a concomitant decrease in the critical uptake required to effect the site-to-pore blockage transition. In turn, this implies that, unless important skeletal rearrangements occur, the nature of the hydrocarbon residues originated from isobutene instead of linear butenes should differ. This issue is addressed in the next section.

DRIFTS Experiments

Four DRIFTS experiments consisting of exposure of the catalyst to a pure isobutene flow at different temperatures and times of exposure were conducted. In this case, we selected feed flow and temperature ranges identical to those used in our previous study. It must be realized that, as H-Ferrierite is a catalyst that presents marked differences in activity between the forward and reverse skeletal isomerization reactions, preservation of all variables inevitably implies different reaction rates. Nevertheless, we elected to use the same temperatures, flow rates, and times of exposure used in our previous *n*-butene-to-isobutene DRIFTS studies.

Figures 7 shows the high-frequency part of the spectra for exposure of the catalyst to isobutene at 573 and 608 K, respectively. For reference, the spectrum of the calcined H-Ferrierite material is shown as curves a. The characteristic acidic O–H stretching signal around 3550–3600 cm^{-1} is evident, as is a minor peak around 3720 cm^{-1} (terminal silanol groups). The C–H stretching region generally spans from 2700 to 3100 cm^{-1}. Specifically, the assignments are $\nu_{as}^{CH_2}$ (aliphatic) ∼ 2930–2940 cm^{-1}, $\nu_{as}^{CH_2}$ (aliphatic) ∼ 2860 cm^{-1}, $\nu_{as}^{CH_3}$ (aliphatic) ∼ 2960–2970 cm^{-1}, $\nu_{as}^{CH_2}$ (olefinic) ∼ 2960 cm^{-1}, and a signal at around 3100 cm^{-1} assigned to free, terminal double bonds, $\nu_{as}^{CH_2}$ (olefinic) (23). In our previous study (3), exposure to 1-butene to progressively higher temperatures and time of exposure caused (i) an overall decrease in intensity of the C–H stretching region, which was ascribed to loss of hydrogen by the hydrocarbon deposits and (ii) a very large relative contribution

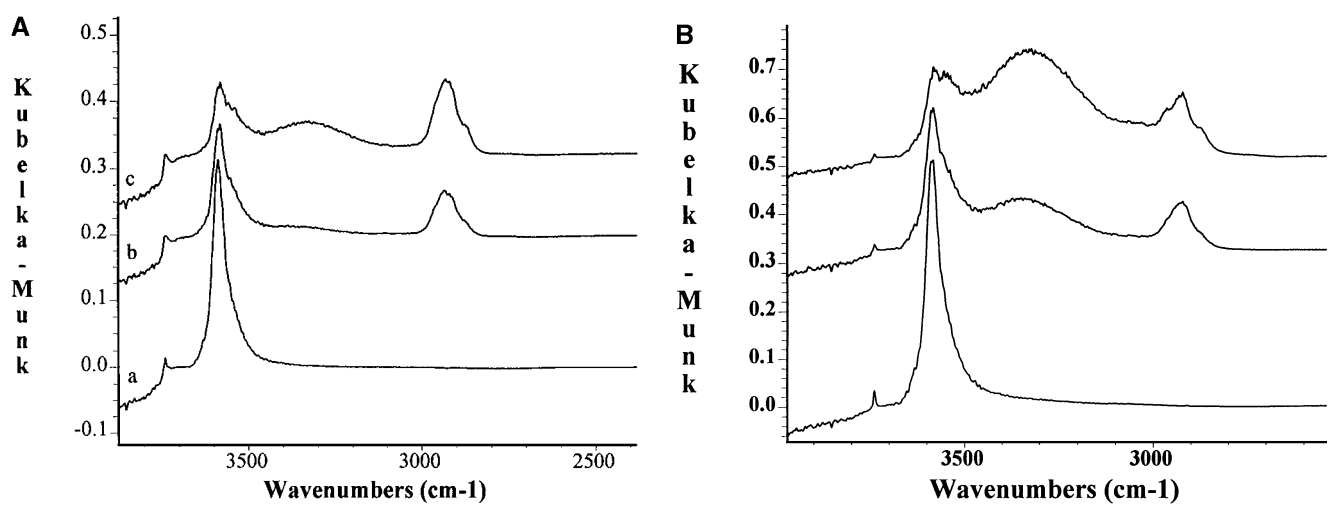

FIG. 7. C–H and O–H stretching region DRIFTS spectra of irreversibly adsorbed isobutene products on H-Ferrierite at (A) 573 K and (B) 608 K. (a) Fresh H-Ferrierite, (b) after 1 h under isobutene, and (c) after overnight exposure to isobutene.

of a band around 2950–3000 cm^{-1} (much larger relative importance at the highest temperature employed, i.e., 608 K). This band was still very noticeable at the lowest temperature and time of exposure used as well. In Fig. 7, it is apparent that such a feature is completely absent when isobutene is used as the DRIFTS cell feed, until it shows as a shoulder of weak intensity at the higest temperature and time of exposure (overnight, 608 K). Thus, as opposed to intrazeolitic polymeric chains generated from 1-butene, we interpret this difference as a limited ability of branched olefin oligomers from isobutene to undergo condensation (cyclization) reactions leading to loss of hydrogen. Zeolite pore size restrictions are expected to play an important role in this process. The broadband around 3300 cm^{-1} (also observed in our previous work with 1-butene) is normally assigned to a perturbation of the acidic O–H by trapped coke species (24), and renders support to the idea that at least an important fraction of the polymeric species reside inside the zeolite pores. As discussed below, coke (in a conventional sense) forms from isobutene at long TOS, but DRIFTS data indicate this process is easier for oligomers from 1-butene.

In Fig. 8, a $\gamma_{C=C}$ signal around 1520 cm^{-1} is evident in all four spectra, indicating that unsaturates still form from isobutene (despite its reduced ability, relative to 1-butene, to do so); also evident is a weak shoulder around 1580 cm^{-1}, normally assigned to microcrystalline polycyclic aromatic stretching. The primary implication of the DRIFTS study of trapped hydrocarbon species is that the "coking" rate analysis discussed in the previous section, which was purposely done within the "kinetic range" of much lower temperatures and much shorter TOS, must simply reflect pore filling by acid-catalyzed polymerization of olefins rather than true coke formation.

Mass Spectrometry

In the temperature and total conversion range employed in this study, the formation of hydrocarbons higher than C_4 from isobutene was found to be essentially negligible. Thus, reliable GC detection became an extremely difficult task with the equipment used in this study. However, valuable qualitative information with respect to the nature of small chain oligomers that are able to desorb at very short TOS can be gained from MS analysis. At this point, it must be emphasized that while formation of coke precursors is obviously a bimolecular process, the isomerization of butenes does not necessarily have to go through the same reaction intermediates. The observation of bimolecular products (e.g., oligomers and disproportionation) is often taken as part of the isomerization network without further analysis. The main goal of this section is to discuss the formation of products at short TOS, especially those that would ultimately lead to coke, without implying that the mere observation of the latter renders support for a bimolecular isomerization mechanism. Figure 9 shows the four most important m/e signals detected in the OBR effluent. The m/e 41 signal primarily tracks all olefins, which in this case are largely dominated by all butene isomers. On the other hand, m/e values of 43, 83, and 97 track formation of octenes and heavier oligomers (25, 26). Mass 43 is also indicative of *n*-butane, a hydrogen transfer product. Mass spectral data for 20 octene isomers from the NIST database were carefully inspected (26). A key feature is that the 83/97 m/e ratio is very large for octenes that would be formed from linear butene dimerization (e.g., linear octenes, 3,4 dimethyl-2-hexene), whereas the same ratio falls sharply for highly branched structures resulting from isobutene dimerization (e.g., trimethylated pentenes). The

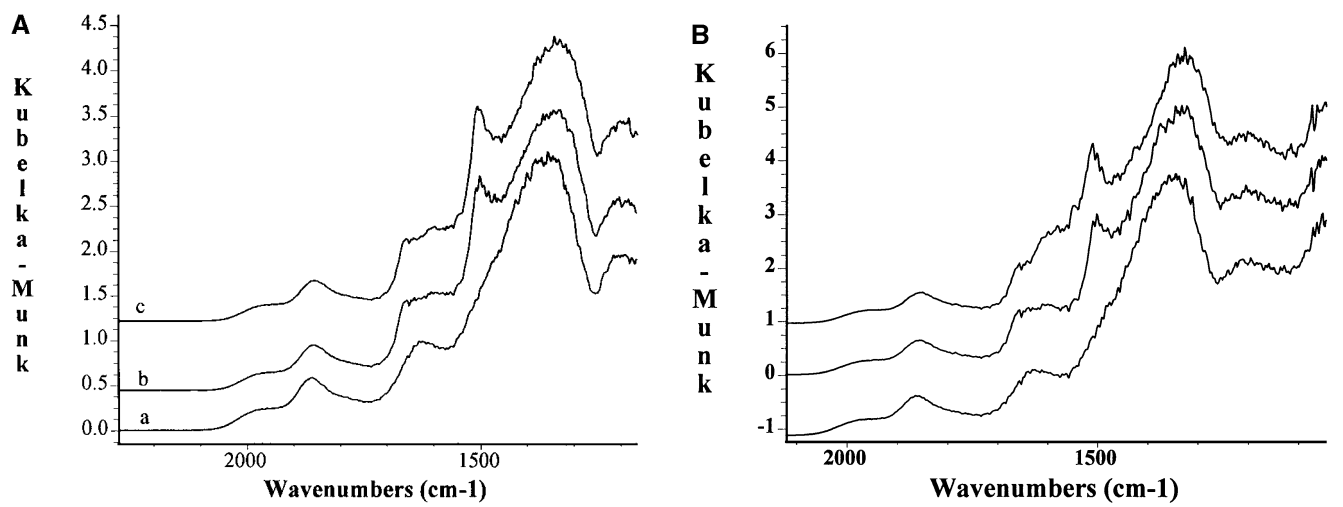

FIG. 8. C=C and C–C stretching and C–H deformation region DRIFTS spectra of irreversibly adsorbed isobutene products on H-Ferrierite at (A) 573 K and (B) 608 K. (a) Fresh H-Ferrierite, (b) after 1 h under isobutene, and (c) after overnight exposure to isobutene.

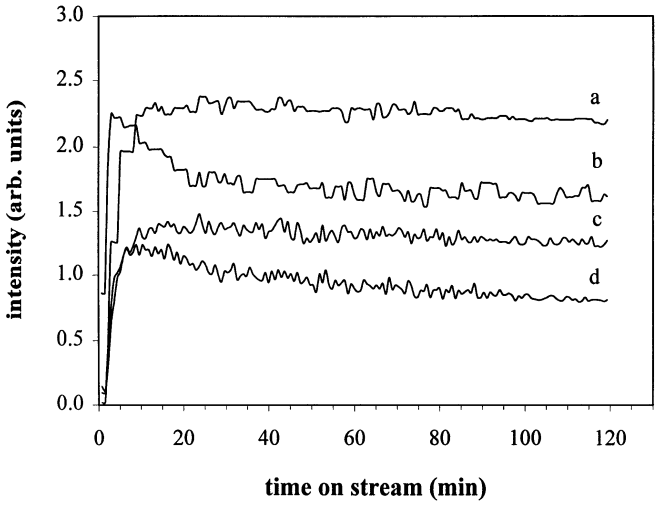

FIG. 9. Relevant mass spectrometer signals from the isobutene product stream at 20.3 kPa, reacting on H-Ferrierite catalyst at 543 K in the OBR cell. WHSV = 37 g isobutene (g cat.)$^{-1}$ h^{-1}, 45 mg H-Ferrierite sample. (a) $m/e = 41 \times 0.05$, (b) $m/e = 43$, (c) $m/e = 97$, (d) $m/e = 83$.

83/97 ratio when 1-butene was used as feed was found to be about 4 : 1 to 5 : 1 (3). Figure 9 shows that the same ratio stabilizes to a value of about 0.6. Thus, there is nearly one order of magnitude difference, and it is clear that highly branched dimers dominate the MS spectrum of octenes when isobutene instead of 1-butene is used as the OBR feed. This implies that heavier (trapped) oligomers formed at short TOS are likely to be highly branched, thereby reducing the carbonaceous residue retention of H-Ferrierite in the so-called site blockage region. Again, this observation regarding isobutene oligomerization does not de facto rule that the isomerization reaction must be bimolecular.

Within error associated with noise in the MS spectra, it is apparent that it takes approximately 10 min to stabilize the m/e 41 (feed) signal. Mass balance done on the OBR reveals that only approximately 1–2% of the hydrocarbon feed is retained during the first 90 s. Figure 9 indicates that the fraction of the feed that appears unaccounted for with respect to the gas phase (MS data) at short TOS must translate into octenes. This behavior resembles that observed in the 1-butene case, i.e., the bed weight also increased much faster than the m/e 41 signal which represents the gas-phase presence of butenes as a lump.

Influence of Adsorbed Oligomer Content on the Isobutene Isomerization Reaction

A large number of experiments were conducted at different temperatures and pressures. A feature common to all of them was that, since most of the oligomer uptake occurs very fast, only runs done at the lowest isobutene partial pressures and temperatures allowed the observation of well-defined rate transients. Thus, the challenge was to find a regime in which transients in both the isomerization and oligomer formation reactions could be monitored under differential reactor conditions. Away from the site blockage region (long TOS), conversion levels and selectivity toward linear butenes became stable, much like in the *n*-butene isomerization case (1, 3). Figure 10 shows the results for two runs at 6.8 kPa isobutene paratial pressure. A nearly linear decay in the linear butene yield is evident at the lowest temperature, which coincides with the linear site blockage region derived from analysis similar to that shown in Fig. 6. As shown in Fig. 10 propene formation falls more rapidly, which indicates that disproportionation and isomerization products are not expected to come from common intermediates even prior to zeolite pore filling. A linear decay of the *n*-butene isomerization rate with oligomer content has also been observed (3). The small increase in isomerization yields with TOS found in catalysts that operate at high conversion level for several minutes (6) is absent when the reaction is operated at low conversions at short TOS, i.e.,

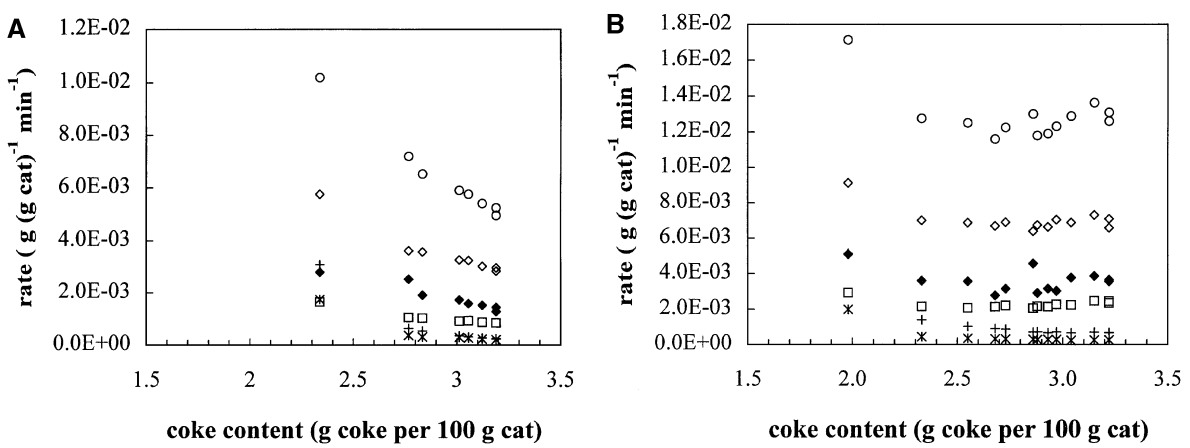

FIG. 10. Rate of product formation in the isobutene isomerization reaction on H-Ferrierite catalyst. WHSV = 12.3 g isobutene (g cat)$^{-1}$ h^{-1}. Isobutene partial pressure in feed: 6.8 kPa at (A) 503 K and (B) 533 K. (○) *n*-butenes as a lump sum, (◇) *trans*-2-butene, (◆) *cis*-2-butene, (□) 1-butene, (∗) isobutane, (+) propene.

when a rate analysis can be carried out. With respect to this issue, our results are consistent with the experiments of Houzvicka and Ponec (4), who showed that the controlled, stepwise generation of hydrocarbon residues does not lead to a maximum in the isomerization rate-versus-TOS curves.

CONCLUSIONS

Oligomerization of isobutene inside the pores of an H-Ferrierite catalyst occurs on a time scale much shorter than that required for true coke formation. The lower critical uptake of coke precursor when isobutene instead of 1-butene is used as reactor feed indicates that (i) pore blockage by highly branched oligomers is particularly effective, and (ii) the bulky nature of isobutene oligomers decreases, with respect 1-butene oligomers, the rate of densification of hydrocarbon residues into true coke-like forms. As in the 1-butene isomerization case, the impact of carbonaceous residue levels on the isobutene isomerization rate is roughly linear at relatively short TOS and does not coincide with the deactivation rate of propene formation even well before the pore blockage mechanism sets in. This implies that (i) selective isobutene isomerization sites do not necessarily operate at the H-Ferrierite pore mouths, (ii) the existence of a "composite" site consisting of some form of preadsorbed hydrocarbon cation onto the acid site is unlikely (no isomerization rate increase with TOS), and (iii) disproportionation and isomerization products do not apear to share a common bimolecular intermediate, even though this could occur between disproportionation and oligomerization species.

In summary, the most probable isomerization mechanisms are shown in Fig. 11. In Fig. 11A, an adsorbed tert-butyl cation serves as the active site for the skeletal rearrangement of a linear butene, leading to a pseudo-monomolecular reaction (6b). Such a site would satisfy the prerequisite that it still possesses a high hydrogen content since as mentioned earlier the time scale of the true coke formation process (benzylic carbocation proposal) does not match that of the rapid transients in the isomerization pathways. However, no improvements in *n*-butene isomerization rates were observed, in both our previous study (3) and the work by Ponec and Houzvicka (4), as a function of time of exposure of the catalyst to a butene feed. It must be emphasized that support for the mechanism shown in Fig. 11A must come from studies in which the amount of coke formed is kept to a minimum (3, 4). This mechanism being autocatalytic, a rate increase with TOS must be demonstrated, but this has not been possible in studies that focus on the behavior of fully coked H-Ferrierite (6). Furthermore, such a network [originally proposed in Ref. (6b)] still suggests that there is a common intermediate for both isomerization and disproportionation. In addition, it is difficult to visualize why this network should operate only for the

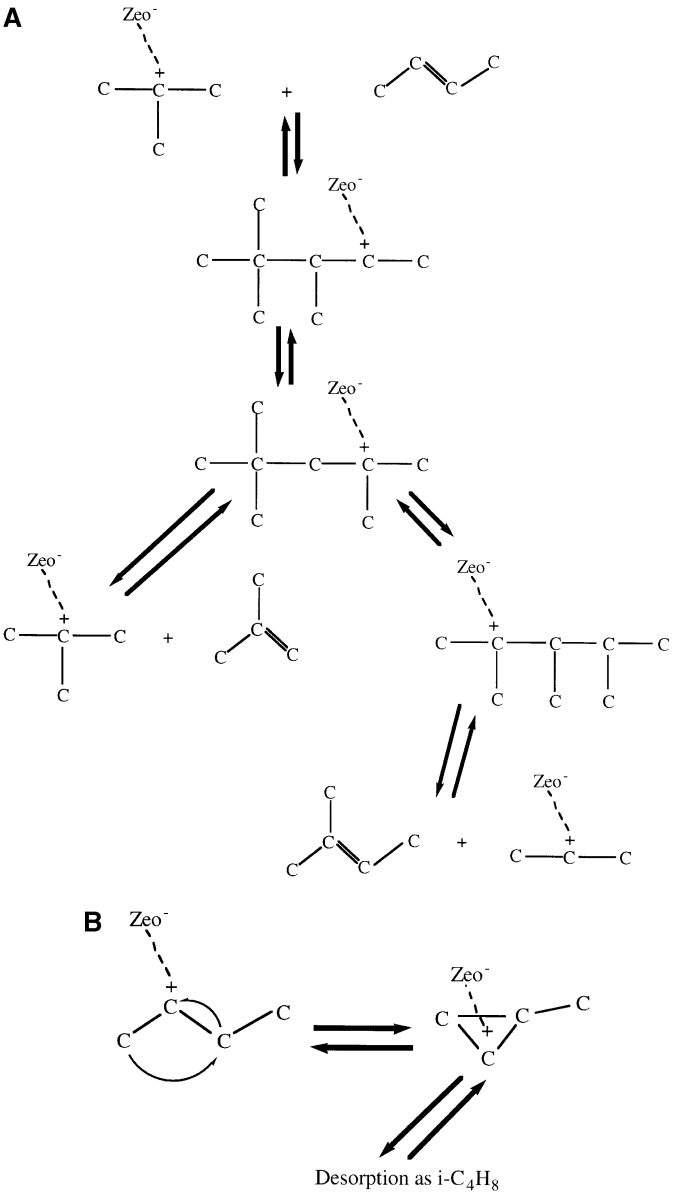

FIG. 11. (A) Pseudomonomolecular and (B) unimolecular mechanisms for *n*-butene isomerization.

n-butene-to-isobutene route but not for the reverse process. We acknowledge that processes such as isotope scrambling in C_4 molecules will progressively become more important as conversion levels are increased, because of the complex and rather reversible network of isomerization, disproportionation, alkylation, and hydrogen transfer reactions. At high conversions, however, it becomes more difficult to ascribe catalyst behavior to a certain reaction mechanism. In Fig. 11B, the unimolecular isomerization pathway is shown. At first sight, it is not appealing from a classic carbocation chemistry viewpoint. It also seems unfavorable in the light of cluster calculations (16), but the precise long-range electrostatic and cage effects of the zeolite lattice on such

species remain an important field in theoretical catalysis. The pathway in Fig. 11B will likely be rejected or supported in the medium-term future, since advances in both theoretical and experimental catalysis are now allowing us to reconsider classic carbocation theories. A third possibility would be that a bimolecular isomerization pathway that differs radically from both oligomerization and disproportionation routes is in effect on H-Ferrierite. Note that the occurrence of reaction orders even lower than unity does not preclude this as a possibility unless the surface dimerization step is rate limiting. Whatever the operating isomerization mechanism, hydrocarbon residues formed during both the forward and reverse $C_4^=$ skeletal isomerization reactions were found to monotonically decrease the rate of formation of butenes and disproportionation species.

ACKNOWLEDGMENTS

We acknowledge a grant from the Nebraska Research Initiative, funding from the National Science Foundation (CTS-9610315) that allowed us to purchase the OBR equipment, and a paid leave of absence for one of us (L.M.P.) from the University of San Juan—Argentina to pursue doctoral studies at the University of Nebraska. We thank R. Gill for help with the OBR apparatus.

REFERENCES

1. Andy, P., Gnep, N. S., Guisnet, M., Benazzi, E., and Travers, C., *J. Catal.* **173**, 322 (1998).
2. Xu, W.-Q., Yin, Y.-G., Suib, S. L., and O'Young C.-L., *J. Phys. Chem.* **99**, 758 (1995).
3. Petkovic, L. M., and Larsen, G., *Ind. Eng. Chem. Res.* **38**, 1822 (1999).
4. Houzvicka, J., and Ponec, V., *Catal. Rev. Sci. Eng.* **39**, 319 (1997).
5. Seo, G., Jeong, H. S., Jang, D.-L., Cho, D. L., and Hong, S. B., *Catal. Lett.* **41**, 189 (1996).
6. (a) Guisnet, M., Andy, P., Gnep, N. S., Benazzi, E., and Travers, C., *J. Catal.* **158**, 551 (1996). (b) Guisnet, M., Andy, P., Boucheffa, Y., Gnep, N. S., Travers, C., and Benazzi, E., *Catal. Lett.* **50**, 159 (1998).
7. Liu, K., Fung, S. C., and Rumschitzki, D. S., *J. Catal.* **169**, 455 (1997).
8. Chen, D., Grønvold, A., Rebo, H. P., Moljord, K., and Holmen, A., *Appl. Catal. A* **137**, L1 (1996).
9. Hershkowitz, F., and Mardiara, P. D., *Ind. Eng. Chem. Res.* **32**, 2969 (1993).
10. Froment, G. F., De Meyer, J., and Derouane, E. G., *J. Catal.* **124**, 391 (1990).
11. Spoto, G., Bordiga, S., Ricchiardi, G., Scarano, D., Zecchina, A., and Borello, E. J., *J. Chem. Soc. Faraday Trans.* **90**, 2827 (1994).
12. Houzvicka, J., and Ponec, V., *Ind. Eng. Chem. Res.* **37**, 303 (1998).
13. Guisnet, M., Andy, P., and Gnep, N. S., *Ind. Eng. Chem. Res.* **37**, 300 (1998).
14. Brouwer, D. M., and Oelderic, J. M., *Rec. Trav. Chim.* **87**, 721 (1968).
15. Brouwer, D. M., and Hogeveen, H., *Prog. Phys. Org. Chem.* **9**, 179 (1972).
16. Rigby, A. M., Kramer, G. J., and van Santen, R. A., *J. Catal.* **170**, 1 (1997).
17. Gill, R., Petkovic, L. M., and Larsen, G., *J. Catal.* **179**, 56 (1998).
18. Larsen, G., Lotero, E., Márquez, M., and Silva, H., *J. Catal.* **157**, 645 (1995).
19. Liu. K., Fung, S. C., Ho, T. C., and Rumchitzki, D. S., *Ind. Eng. Chem. Res.* **36**, 3264 (1997).
20. Thomas, J. M., and Thomas, W. J., "Principles and Practice of Heterogeneous Catalysis," p. 304. VCH, Cambridge, 1997.
21. Perry, R. H., and Green, D. W., "Perry's Chemical Engineers' Handbook," 7th ed. Sect. 2–196. McGraw–Hill, New York, 1997.
22. Choudary, V. R., *Chem. Ind. Dev.* **8**, 32 (1974).
23. Nyquist, R. A., "The interpretation of Vapor Phase Infrared Spectra," Sadtler Research Laboratories, PA, 1984.
24. Karge, H. G., *Stud. Surf. Sci. Catal.* **58**, 531 (1991).
25. Cornu, A., and Massot, R., "Compilation of Mass Spectral Data," Vol. 1, 2nd ed. Heyden, London, 1975.
26. NIST Webbook, URL http://webbook.nist.gov.